
Efficient Bayesian Updates for Deep Learning via Laplace Approximations

Denis Huseljic* Marek Herde Lukas Rauch Paul Hahn Zhixin Huang
 Daniel Kottke Stephan Vogt Bernhard Sick
 University of Kassel, Intelligent Embedded Systems
 *dhuseljic@uni-kassel.de

Abstract

Since training deep neural networks takes significant computational resources, extending the training dataset with new data is difficult, as it typically requires complete retraining. Moreover, specific applications do not allow costly retraining due to time or computational constraints. We address this issue by proposing a novel Bayesian update method for deep neural networks by using a last-layer Laplace approximation. Concretely, we leverage second-order optimization techniques on the Gaussian posterior distribution of a Laplace approximation, computing the inverse Hessian matrix in closed form. This way, our method allows for fast and effective updates upon the arrival of new data in a stationary setting. A large-scale evaluation study across different data modalities confirms that our updates are a fast and competitive alternative to costly retraining. Furthermore, we demonstrate its applicability in a deep active learning scenario by using our update to improve existing selection strategies.

1 Introduction

Training deep neural networks (DNNs) often demands significant time and computational resources. Moreover, when extending a dataset with new data, DNNs require complete retraining, which involves both the new and previously used data to prevent issues such as catastrophic forgetting [42]. Although improved generalization performance typically justifies exhaustive retraining, it may not always be feasible immediately after new data arrives. Key scenarios where retraining is beneficial but impractical include: (1) When data arrives sequentially and an immediate update is necessary, e.g., in active learning (AL) [48] or when working on data streams [46], (2) when only limited computational resources are available, e.g., training on embedded hardware [51], and (3) when there are privacy concerns, which restrict sharing new data with distributed computing units [51]. In these scenarios, it is crucial to devise methods that allow DNNs to incorporate new data fast and effectively.

While numerous studies developed methods to update DNNs effectively [19, 42, 50], these methods typically assume a non-stationary setting in which the respective data distribution changes over time [52]. As a result, these methods often focus on situations where new data arrives in relatively large amounts [42], neglecting scenarios where an immediate update with a small number of instances might be beneficial. In contrast, we assume a *stationary setting* with the goal to *immediately* update the model upon the arrival of new data, even in the case of a single data point.

As an example scenario, we consider AL throughout this article. A popular approach in AL is to use a one-step-look-ahead to select instances that significantly change model predictions [44, 50]. This approach assesses how model predictions would change, when including a specific instance in the labeled pool and updating the model. Consequently, it requires a highly efficient update

*Corresponding Author

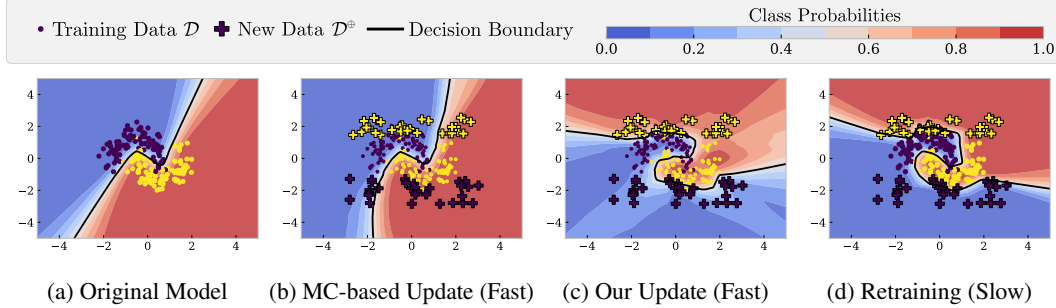


Figure 1: Comparison of different BNNs on the two moons dataset. (a) The original model resulting from training on the original dataset. (b) The typical MC-based update applied to the original model [21, 50]. (c) Our update applied to the original model. (d) The model resulting from retraining on both the original and the new dataset.

method, as it involves updates for all candidates of a large dataset. To make this feasible, several AL selection strategies utilize a Bayesian neural network (BNN) and rely on Monte Carlo (MC)-based updates [50]. However, while this update is fast, it falls short in performance compared to a retrained model (cf. Fig. 1). In such a scenario, a fast *and* effective update would enhance these strategies.

In this article, we propose a novel Bayesian update method. Like [50, 42, 21], we consider BNNs since they are particularly well-suited for our setting. The posterior distribution can be updated in a theoretically sound way by treating it as the prior distribution when new data becomes available. However, instead of relying on MC-based BNNs (e.g., MC-Dropout), we transform an arbitrary DNN into a BNN by employing a last-layer Laplace approximation (LA) [7], giving us a closed-form expression for the posterior distribution. Then, we leverage second-order optimization techniques on the Gaussian posterior distribution of the LA. To ensure low computational complexity, we compute the required inverse Hessian in closed form. The resulting update is both fast – it can be used in the previously described scenarios – and effective – its performance closely aligns with retraining. Moreover, our update can be combined with more recently developed BNNs such as Spectral Normalized Neural Gaussian Process (SNGP) [30].

Extensive studies across different data modalities, including image and text datasets, demonstrate that our updates outperform the typically employed MC-based ones [21, 50] in terms of speed and performance. Further, to demonstrate the applicability in one of the previously mentioned scenarios, we revisit AL and propose a simple and effective idea to improve existing selection strategies by immediately making use of acquired labels.

Contributions

- We propose a novel update method for DNNs by employing a last-layer LA and second-order optimization techniques, suitable for scenarios where data arrives in small quantities, and immediate model updates are required.
- We conduct a comprehensive evaluation of our update method across different data modalities, demonstrating superior performance and speed compared to the MC-based updates.
- We propose a simple framework to improve existing AL strategies employing our updates.

2 Related Work

Similar to our setting, **continual learning** [8] updates models by exclusively training with data from a new task, addressing the challenge of retaining knowledge from previously learned tasks. Popular techniques [42, 19] use conventional first-order optimization methods, incorporating a regularization term to counteract catastrophic forgetting. More specifically, [42] and [19] derive a regularization term from an LA that penalizes large deviations from prior knowledge. Ebrahimi et al. [11] exploit uncertainty estimates of BNNs to dynamically adjust learning rates during training. Unlike our method, these approaches require training over multiple epochs, preventing immediate updates.

Additionally, they require large amounts of new data (thousands of data points) per task, whereas our update method is designed for smaller datasets, ranging from single to hundreds of data points. More closely related to our work is **online learning** [17], which aims to sequentially and efficiently update models from incoming data streams. Traditional approaches often focus on linear [57, 6] or shallow [22, 45] models with maximum-margin classification. However, applying online learning to DNNs remains difficult due to issues such as convergence, vanishing gradients, and large model sizes [46, 27]. To address these challenges, Sahoo et al. [46] proposed a method that modifies a DNN’s architecture to facilitate updates. We argue that this approach is restrictive in state-of-the-art settings, given the increasing reliance on pretrained architectures. Most similar to our setting is the work on Bayesian online inference by Kirsch et al. [21]. The core idea is to sample hypotheses, e.g., via MC-Dropout, from the posterior distribution of a BNN and weight their importance according to the respective likelihoods for sequentially arriving data. We refer to these types of updates as MC-based updates. The empirical results raised concerns regarding the applicability of such MC updates in high-dimensional parameter spaces.

BNNs [53, 12] induce a prior distribution over their parameters, i.e., weights, and learn a posterior distribution given training data. Predictions are made by marginalizing this posterior. BNN types differ mainly in their probabilistic model and sampling from the posterior distribution [18]. MC-Dropout [13], one of the most prominent BNN types, is a regularization technique performed during training. Using dropout during evaluation, called MC-Dropout, we obtain a distribution for the predictions corresponding to a variational distribution in the parameter space. Due to its simplicity and training efficiency, MC-Dropout is often used for comparison. However, its inference is inefficient and predictions may not properly represent uncertainty estimates [37]. Deep ensembles [25] consist of multiple DNNs. Combined with regularization, these DNNs are samples (different modes) of the parameters’ posterior distribution. Ensembles typically provide better uncertainty estimates than MC-Dropout but require more computational capacity during training [37]. A BNN obtained via LA [43] is computationally more efficient than MC-Dropout and deep ensembles. It specifies an approximate Gaussian posterior distribution, where the maximum a posteriori (MAP) estimate defines the mean and the inverse of the negative log posterior’s Hessian at the MAP estimate corresponds to the covariance matrix. As computing this Hessian is expensive for large DNNs, LA is often used only in the last layer [7]. SNGP [30] combines LA with random Fourier features [38] and spectral normalization [34] to approximate a Gaussian process.

AL poses significant challenges in practice due to the computational cost associated with required retraining per cycle. The emergence of one-step-look-ahead strategies [44, 50, 56] further highlights the importance of efficient model updates. Notably, BEMPS [50] evaluates all possible candidates (i.e., instances) in a dataset to select those that are anticipated to alter the model’s predictions substantially. However, this strategy utilizes an MC-based BNN with deep ensembles, relying on MC-based updates. They assume that all hypotheses are equally likely to explain the data before an update step. While this update is fast, its performance is inferior to that of a retrained model.

3 Fast Bayesian Updates for Deep Neural Networks

In this section, we present our new Bayesian update method. First, we introduce the general concept of Bayesian updates and the commonly applied MC-based Bayesian updates [21, 50]. Afterward, we propose our novel method focusing on an efficient update of the Gaussian posterior distribution via last-layer LAs. For an introduction to LA, we refer to [7].

3.1 Bayesian Updates

We focus on classification problems with instance space \mathcal{X} and label space $\mathcal{Y} = \{0, \dots, K-1\}$. The primary goal in our setting is to efficiently incorporate the information of new instance-label pairs $\mathcal{D}^\oplus = \{(\mathbf{x}_n, y_n)\}_{n=1}^N \subset \mathcal{X} \times \mathcal{Y}$ into a BNN trained on dataset $\mathcal{D} \subset \mathcal{X} \times \mathcal{Y}$. Retraining the entire network on the extended dataset $\mathcal{D} \cup \mathcal{D}^\oplus$ results in high computational cost for a large dataset \mathcal{D} . Conversely, using the new data solely can cause catastrophic forgetting [42].

For this purpose, we employ BNNs [12] with Bayesian updates [35] as an efficient alternative to retraining. The main idea of BNNs is to estimate posterior distribution $p(\omega|\mathcal{D})$ over the parameters $\omega \in \Omega$ given the observed training data \mathcal{D} using Bayes’ theorem. The obtained posterior distribution over the parameters can then be used to specify the predictive distribution over a new instance’s class

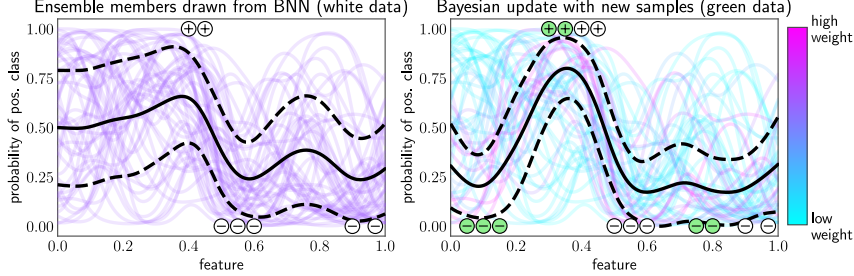


Figure 2: The left plot shows the predicted probabilities of the positive class for each hypothesis (colored lines) drawn from a BNN as well as the mean (black solid line) and standard deviation (black dashed line) of its predictive distribution. The right plot shows updated weights for each hypothesis and the predictive distribution after observing additional instances (green).

membership via marginalization:

$$p(y|\mathbf{x}, \mathcal{D}) = \mathbb{E}_{p(\omega|\mathcal{D})}[p(y|\mathbf{x}, \omega)] = \int p(y|\mathbf{x}, \omega)p(\omega|\mathcal{D}) d\omega. \quad (1)$$

Thereby, the likelihood $p(y|\mathbf{x}, \omega) = [\text{softmax}(f^\omega(\mathbf{x}))]_y$ denotes the probabilistic output of a DNN with parameters ω , where $f^\omega : \mathcal{X} \rightarrow \mathbb{R}^K$ is a function outputting class-wise logits.²

The formulation in Eq. (1) provides a theoretically sound way to obtain updated predictions. In particular, this is because the probabilistic outputs $p(y|\mathbf{x}, \omega)$ do not directly depend on the training data \mathcal{D} . Consequently, to obtain an updated predictive distribution, we do not need to update the parameters ω directly but only the posterior distribution $p(\omega|\mathcal{D})$. The updated posterior distribution $p(\omega|\mathcal{D}, \mathcal{D}^\oplus)$ is found through Bayes' theorem, where the current posterior distribution $p(\omega|\mathcal{D})$ is considered the prior and multiplied with the likelihood $p(y|\mathbf{x}, \omega)$ per instance-label pair $(\mathbf{x}, y) \in \mathcal{D}^\oplus$. As instances in \mathcal{D} and \mathcal{D}^\oplus are assumed to be independently distributed, we can simplify the likelihood and reformulate the parameter distribution as follows³:

$$p(\omega|\mathcal{D}^\oplus, \mathcal{D}) \propto p(\omega|\mathcal{D})p(\mathcal{D}^\oplus|\mathcal{D}, \omega) \stackrel{\text{i.i.d.}}{=} p(\omega|\mathcal{D})p(\mathcal{D}^\oplus|\omega) = p(\omega|\mathcal{D}) \prod_{(\mathbf{x}, y) \in \mathcal{D}^\oplus} p(y|\mathbf{x}, \omega). \quad (2)$$

We refer to Eq. (2) as the Bayesian update.

The most common realization [21, 50] of this update is through MC-based BNNs, such as MC-Dropout and deep ensembles. These BNNs rely on samples (or hypotheses) $\omega_1, \dots, \omega_M$ drawn from an approximate posterior $q(\omega|\mathcal{D})$. Research [56, 50] assumes that all hypotheses are equally likely to explain the observed data and have the same probability before updating. By updating the posterior distribution through Eq. (2), they weigh more likely hypotheses given the new data higher. We refer to these as MC-based updates with a formal definition given in Appendix A. Figure 2 illustrates this concept where different hypotheses $\omega_1, \dots, \omega_M \sim q(\omega|\mathcal{D})$ are shown. Each hypothesis represents a possible true solution for the learning task (white instances). When new data (green instances) arrives, we weigh each hypothesis by its likelihood of explaining the new data and obtain an updated prediction without retraining. This results in an updated predictive distribution, as seen in bold in Fig. 2 (right).

3.2 Fast Approximations of Bayesian Updates for Deep Neural Networks

Our update method is based on a combination of two concepts. First, instead of MC-based BNNs, we suggest using LAs on the last layer of a DNN. Second, we directly modify the approximate posterior distribution of the LA, providing a much more flexible way to adapt it to new data than reweighting. In the following, we explain each component in detail. For now, we focus on binary classification with $K = 2$, and refer to Appendix C for an extension to multi-class classification.

Last-layer LA: LAs approximate the (intractable) posterior distribution $p(\omega|\mathcal{D})$ with a Gaussian centered on the maximum a posteriori (MAP) estimate with a covariance equal to the negative Hessian

²We denote the i -th element of a vector \mathbf{b} as $[\mathbf{b}]_i = b_i$.

³We denote $p(y_1, \dots, y_N \mid \mathbf{x}_1, \dots, \mathbf{x}_N, \omega)$ with $\mathcal{D} = \{(\mathbf{x}_n, y_n)\}_{n=1}^N$ as $p(\mathcal{D}|\omega)$.

of the log posterior [7]. We denote this approximate distribution as

$$q(\boldsymbol{\omega}|\mathcal{D}) = \mathcal{N}(\boldsymbol{\omega}|\hat{\boldsymbol{\mu}}, \hat{\boldsymbol{\Sigma}}) \approx q(\boldsymbol{\omega}) \prod_{(\mathbf{x}, y) \in \mathcal{D}} p(y|\mathbf{x}, \boldsymbol{\omega}), \quad (3)$$

where $q(\boldsymbol{\omega})$ is a Gaussian prior distribution. The MAP estimate $\hat{\boldsymbol{\mu}}$ results from training on \mathcal{D} with conventional gradient optimization techniques. The covariance matrix $\hat{\boldsymbol{\Sigma}}$ is the inverse Hessian of the negative log posterior evaluated at the MAP estimate $\hat{\boldsymbol{\mu}}$ given training data \mathcal{D} . We model the posterior distribution only on the last layer of a DNN to ensure fast inference.

The benefits of using a last-layer LA are manifold. Given access to $q(\boldsymbol{\omega}|\mathcal{D})$ through a Gaussian, we enable *more flexible updates* by being able to modify the mean and covariance directly. In contrast, MC-based updates only change the approximate distribution by reweighting hypotheses, leading to a strong dependency on the samples $\boldsymbol{\omega}_1, \dots, \boldsymbol{\omega}_M$. Last-layer LAs can be *integrated seamlessly* into nearly all DNNs, including pretrained models, as only the covariance has to be computed to obtain $q(\boldsymbol{\omega}|\mathcal{D})$. Finally, compared to deep ensembles and MC-Dropout, last-layer LAs introduce *minimal computational overhead*. While deep ensembles require longer training and MC-dropout impairs the inference time, LAs simply need to calculate a covariance matrix after training and allow fast inference (cf. Eq. (1)) through techniques such as mean-field approximation [32].

Second-Order Update: The second concept focuses on the update step of the Gaussian distribution. When observing new data, we follow the same approach as in Eq. (3), but with $q(\boldsymbol{\omega}|\mathcal{D})$ as our prior:

$$q(\boldsymbol{\omega}|\mathcal{D}, \mathcal{D}^\oplus) = \mathcal{N}(\boldsymbol{\omega}|\hat{\boldsymbol{\mu}}^{\text{upd}}, \hat{\boldsymbol{\Sigma}}^{\text{upd}}) \approx q(\boldsymbol{\omega}|\mathcal{D}) \prod_{(\mathbf{x}, y) \in \mathcal{D}^\oplus} p(y|\mathbf{x}, \boldsymbol{\omega}), \quad (4)$$

where $\hat{\boldsymbol{\mu}}^{\text{upd}}$ and $\hat{\boldsymbol{\Sigma}}^{\text{upd}}$ represent the updated mean and covariance, respectively. The resulting updated posterior $q(\boldsymbol{\omega}|\mathcal{D}, \mathcal{D}^\oplus)$ is non-Gaussian due to $p(y|\mathbf{x}, \boldsymbol{\omega})$ being a categorical likelihood. Consequently, the closed-form computation of the integral in Eq. (1) becomes intractable. The basic idea of our update is to approximate the new posterior $q(\boldsymbol{\omega}|\mathcal{D}, \mathcal{D}^\oplus)$ by first applying a second-order optimization step via Gauss-Newton and then estimating the new covariance at that point. Thus, the updated mean and covariance are given by:

$$\hat{\boldsymbol{\mu}}^{\text{upd}} = \hat{\boldsymbol{\mu}} - \gamma \mathbf{H}^{-1}(\hat{\boldsymbol{\mu}}, \hat{\boldsymbol{\Sigma}}, \mathcal{D}^\oplus) \sum_{(\mathbf{x}, y) \in \mathcal{D}^\oplus} (p_{\mathbf{x}} - y) \mathbf{h}_{\mathbf{x}}, \quad (5)$$

$$\hat{\boldsymbol{\Sigma}}^{\text{upd}} = \mathbf{H}^{-1}(\hat{\boldsymbol{\mu}}^{\text{upd}}, \hat{\boldsymbol{\Sigma}}, \mathcal{D}^\oplus), \quad (6)$$

where $\mathbf{h}_{\mathbf{x}}$ denotes the representation of \mathbf{x} at the penultimate layer, $p_{\mathbf{x}} = \text{sigmoid}(\mathbf{h}_{\mathbf{x}}^\top \boldsymbol{\mu})$ is the probability for the positive class, and γ is a factor controlling the step size. The required updated Hessian can be computed efficiently in closed form following [49] by

$$\mathbf{H}^{-1}(\boldsymbol{\mu}, \boldsymbol{\Sigma}, \mathcal{A}) = \boldsymbol{\Sigma} - \sum_{(\mathbf{x}, y) \in \mathcal{A}} \frac{p_{\mathbf{x}}(1 - p_{\mathbf{x}})}{1 + \bar{\sigma}_{\mathbf{x}} \cdot p_{\mathbf{x}}(1 - p_{\mathbf{x}})} (\boldsymbol{\Sigma} \mathbf{h}_{\mathbf{x}}) (\boldsymbol{\Sigma} \mathbf{h}_{\mathbf{x}})^\top, \quad (7)$$

where $\bar{\sigma}_{\mathbf{x}} = \mathbf{h}_{\mathbf{x}}^\top \boldsymbol{\Sigma} \mathbf{h}_{\mathbf{x}}$ is the predictive variance. The derivation can be found in Appendix D.

The idea behind using second-order optimization techniques is that they are more robust than first-order gradient optimization techniques due to the incorporation of curvature information of the log posterior. This results in a more accurate representation of the loss landscape, leading to improved parameter updates. A critical aspect of our method's efficiency is that we do not need to recompute the Hessian from scratch. Instead, our updates leverage the covariance available through LAs and use the Woodbury identity [55] for closed-form inversion, significantly reducing computational overhead. Further, a common problem with last-layer LAs is that the Hessian can become a bottleneck when dealing with a large number of classes. To address this, we can approximate the Hessian in Eq. (7) by considering a Gaussian likelihood instead of a multi-class one, as also done in [30, 12].

4 Bayesian Updating Experiments

In this section, we evaluate the effectiveness and speed of the proposed update by comparing it against competitors on various benchmark datasets for image and text classification. Our code is publicly available at <https://github.com/dhuseljic/dal-toolbox>.

4.1 Experimental Setup

Our **experimental design** is based on the work of [21]. First, we train a DNN on the training dataset \mathcal{D} (baseline). We then use this baseline DNN to perform a last-layer LA and different Bayesian updates on additional instance-label pairs \mathcal{D}^\oplus and compare these results to retraining the DNN on the complete dataset $\mathcal{D} \cup \mathcal{D}^\oplus$. To ensure a comprehensive evaluation, we evaluate i) the influence of the step size γ on chosen validation datasets, ii) the impact of our update at different learning stages of the DNN, iii) the impact of our update with increasing sizes of new arriving datasets, and iv) the time-efficiency of our update by considering the speed-up factor against competitors. For comparison, we consider MC-based updates by sampling 10k hypotheses from the approximate Gaussian posterior $q(\omega|\mathcal{D})$ and the less complex first-order updates only considering gradients (cf. Appendix A). Since the latter does not use the Hessian, this comparison allows us to assess the benefits of using second-order optimization. Moreover, we exclude retraining solely on \mathcal{D}^\oplus , as we empirically found that it leads to catastrophic forgetting [19]. For reproducibility, we average all performance metrics across 10 repetitions.

The datasets \mathcal{D} and \mathcal{D}^\oplus are randomly sampled from real-world datasets. We use three image and three text **benchmark datasets** commonly used in literature [16, 39] with varying complexity reflected through different numbers of classes. Table 1 gives an overview. A detailed summary for each dataset is provided in Appendix E.

The goal of an update method is to ensure both effectiveness and speed. To assess this, we use different **performance metrics**. For evaluating effectiveness, or how well an update or retraining generalizes, we measure accuracy. When experimenting with hyperparameters, accuracy is assessed on a 10% validation split. Otherwise, it is measured on the test dataset. An optimal update method should achieve the same performance as completely retraining the DNN with $\mathcal{D} \cup \mathcal{D}^\oplus$. To assess the speed of an update, we report the speed-up factor compared to retraining by dividing the time required for retraining by the time required for updating. Retraining and updating times were recorded on an NVIDIA RTX 4090 GPU and an AMD Ryzen 9 7950X CPU, respectively.

We choose commonly employed DNN **architectures** from the literature [16, 50]. For image datasets, we employ a Vision Transformer (ViT) [10] with pretrained weights via self-supervised learning, complemented by a randomly initialized fully connected layer. Specifically, we use the DINOv2-ViT-S/14 model [36] with a feature dimension of $D = 384$ in its final hidden layer. For text datasets, we employ the transformer-based pre-trained language model BERT [9]. We utilize BERT-BASED-UNCASED from the Huggingface library [54] with the [CLS] token as the embedding of an instance with a feature dimension of $D = 768$ and a maximum sequence length of 512. We train each DNN by finetuning for 200 epochs, employing the Rectified Adam optimizer [31] with a training batch size of 64, a learning rate of 0.01 for images and 0.1 for text, and weight decay of 0.0001. In addition, we utilize a cosine annealing learning rate scheduler. These hyperparameters were determined empirically to be effective across all datasets by investigating the loss convergence on validation splits.

4.2 Experiments

Hyperparameter Ablation: In Eq. (5), we introduced the hyperparameter γ , which controls the step size of our update. Intuitively, this factor determines the extent to which the DNN is influenced by the new dataset \mathcal{D}^\oplus . This factor is essential to control the update process and avoid issues such as catastrophic forgetting. Similarly, first-order and MC-based updates also utilize this factor to mitigate such problems. For further details, we refer to Appendix A.

To investigate the influence of γ and determine a suitable value for all subsequent experiments, we conduct a simple ablation study on two datasets. The results of our update are shown here, while the results for first-order and MC-based updates can be found in Appendix B. We determine the value of γ in this manner since an extensive hyperparameter search for update methods is typically impractical in an online setting [8]. Hence, fixing a value beforehand is necessary. We randomly sample an initial dataset \mathcal{D} of 50 instances and train our baseline DNN. Subsequently, updates and retraining

Table 1: Overview of datasets.

Type	Dataset	Reference	# classes
Image	Cifar-10	[24]	10
	Snacks	[33]	20
	DTD	[5]	49
Text	DBPedia	[2]	14
	Banking-77	[4]	77
	Clinic-150	[26]	150

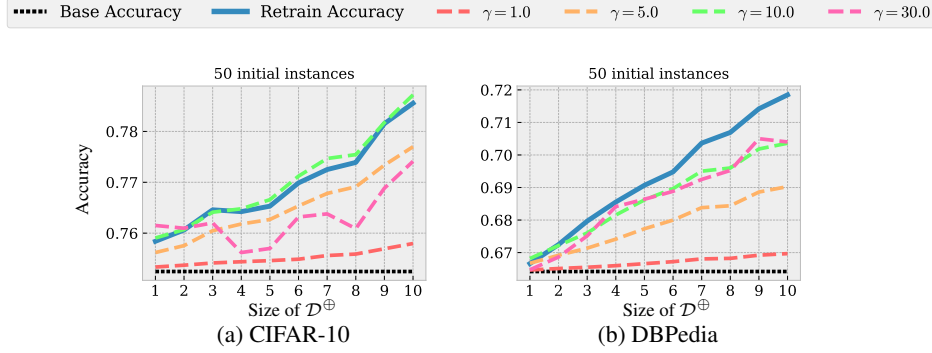


Figure 3: Accuracies after updating with different values for γ in comparison to the baseline DNN and retraining.

are performed on randomly sampled datasets $|\mathcal{D}^\oplus| \in \{1, \dots, < 10\}$, and the accuracy is computed on a validation split. We repeat this process for different values of γ .

The resulting curves in Fig. 3 indicate that our update with \mathcal{D}^\oplus consistently achieves better performance than the baseline DNN that is only trained on \mathcal{D} . For both CIFAR-10 and DBpedia, updating with $\gamma = 1$ does not yield accuracies close to retraining, suggesting that the update is too weak. By increasing γ , we observe accuracies much closer to complete retraining, with $\gamma = 10$ being sufficient for CIFAR-10 and DBpedia. For CIFAR-10, we also notice that a very high value, i.e., $\gamma = 30$, can lead to worse performance, likely due to catastrophic forgetting. To ensure effective updates across all datasets, we will be using $\gamma = 10$ in all subsequent experiments. While this may not be optimal for some datasets, it should ensure a consistently working update process in all cases.

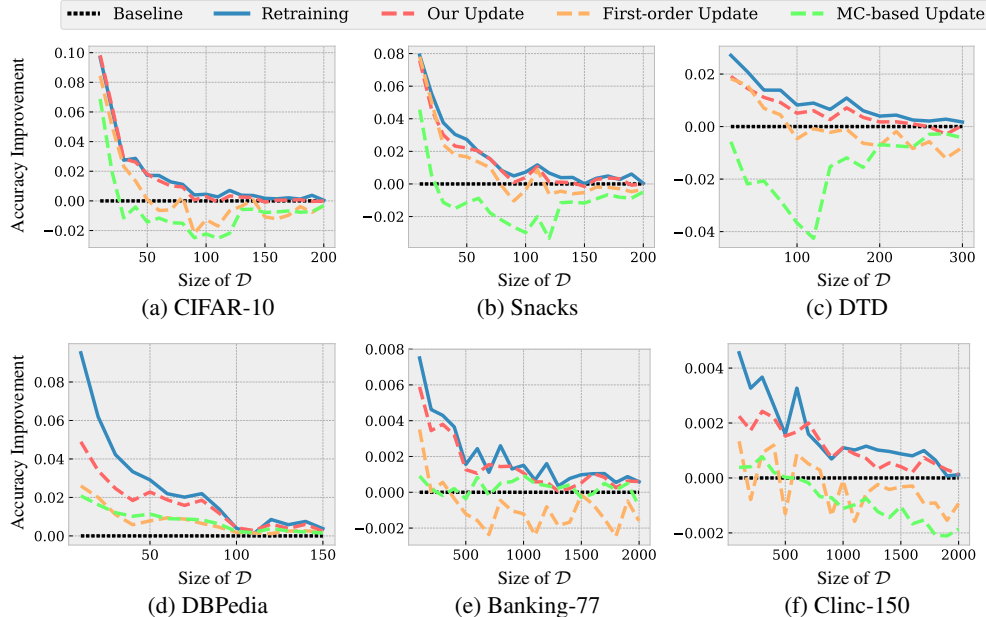


Figure 4: Accuracy improvement curves for six benchmark datasets, showing the difference in accuracy between retrained and updated DNNs for varying sizes of \mathcal{D} .

Different Learning Stages: To investigate how our update behaves at different stages of learning, we train the baseline DNN on varying sizes of initial datasets \mathcal{D} and update it with a new dataset of fixed size $|\mathcal{D}^\oplus| = 10$. To better visualize the differences, we report accuracy improvement of updated/retrained DNNs relative to the baseline in Fig. 4. The results demonstrate that our updates provide the highest accuracy improvements across all datasets, highlighting the effective and consistent performance improvements of our update at different stages of learning. While first-order

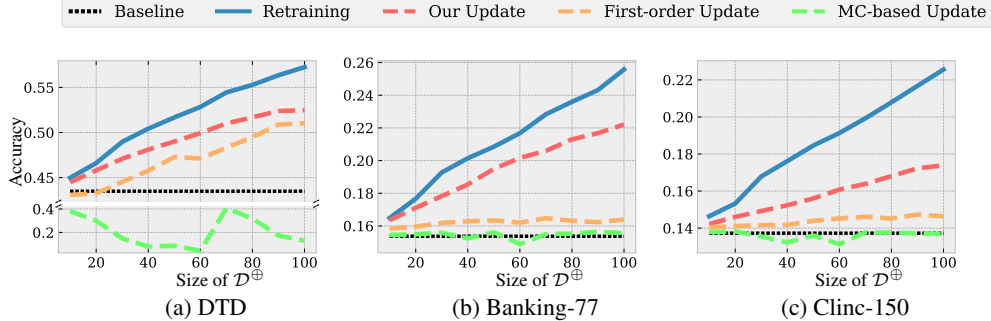


Figure 5: Accuracy curves for three benchmark datasets after updating and retraining DNNs for varying sizes of \mathcal{D}^\oplus .

and MC-based updates are also effective in earlier stages (when $|\mathcal{D}| < 50$), they tend to be less effective and even deteriorate accuracy in later stages. Compared to the first-order update, our update consistently enhances performance due to including the Hessian. As the Hessian considers curvature information about the posterior, the update is more robust regarding the choice of γ .

Varying Size of \mathcal{D}^\oplus : To investigate our update’s behavior with an increasing number of new data points in \mathcal{D}^\oplus , we train a baseline DNN with a fixed initial dataset $|\mathcal{D}| = 100$ and vary the size of the new dataset $|\mathcal{D}^\oplus| \in \{10, 20, \dots, 100\}$. We report the results for the most complex datasets DTD, Banking-77 and Clinc-150. In Fig. 5 we observe that as the size of \mathcal{D}^\oplus increases, the accuracy of retraining, our update, and the first-order update consistently improves. In contrast, MC-based updates result in worse accuracies than the baseline, indicating that it is not suited for an increasing size of \mathcal{D}^\oplus . Considering our update, we see that it consistently achieves better accuracies compared to competitors, regardless of the complexity of the dataset. Moreover, first-order updates seem to be less effective on the more complex datasets such as Banking-77 and Clinc-150, highlighting the importance of the Hessian.

Time Comparison: Finally, to evaluate the speed of our update, we fix the size of the new dataset to $|\mathcal{D}^\oplus| = 10$ and compute the speed-up relative to retraining by varying the initial dataset size $|\mathcal{D}|$. Figure 6 presents the speed-up factors of all update methods on CIFAR-10. All methods are faster than retraining, with the first-order update being the fastest. For example, with an initial dataset size of $|\mathcal{D}| = 1000$, the first-order update is about 1700 times faster than retraining. Notably, our update provides a similar speed-up factor while yielding more effective updates by using the closed-form update of the Hessian. Compared to MC-based updates, both the first-order and our update are significantly faster.

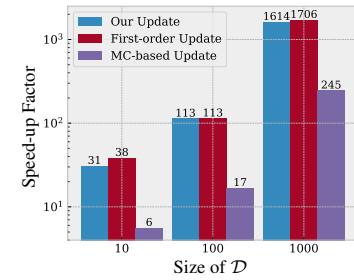


Figure 6: Speed-up of update methods compared to retraining.

5 Use Case: Deep Active Learning

To demonstrate the potential of our proposed update in a practical setting, we return to deep AL [48], where a selection strategy iteratively selects unlabeled instances to be labeled by an oracle. This selection is based on information provided by a DNN trained on the currently available labeled instances. The goal is to maximize the DNN’s performance while minimizing the number of label acquisitions. In the deep learning setting, instances are typically chosen in batches to reduce the number of retraining processes after a selection step [20].

The naive idea of using sequential selection strategies for batch selection is to use the top- b instances. As this might cause a lack of diversity between selected instances, batch selection strategies have been proposed to solve this problem [47, 1, 20]. Our idea is to overcome the necessity of batch strategies by using the proposed update method with sequential selection strategies as a fast alternative to retraining. After acquiring b labels, we retrain the DNN similar to batch selection strategies. An algorithm implementing this idea can be found in Appendix F. The hypothesis is that our idea achieves

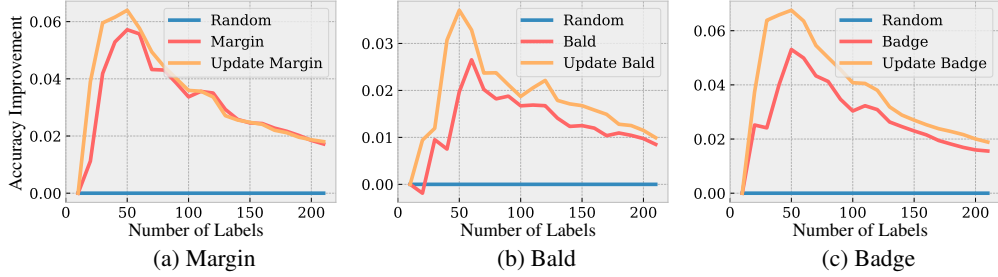


Figure 7: Accuracy improvement curves showing the difference in accuracy between the respective selection strategy and random instance selection.

higher performance compared to selecting the top- b instance for already well-performing sequential selection strategies [41], which are Margin [3] and BALD [14]. Additionally, we are interested in whether our idea can act as a replacement for the diversity component of batch selection strategies. Therefore, we also evaluate the popular strategy Badge [1] in combination with our updates.

For this use case, we choose the CIFAR-10 dataset with a label budget of $B = 200$, an acquisition size of $b = 10$ instances, and the same DNN architecture as in our previous experiments (cf. Section 4). Figure 7 shows the accuracy improvement curves relative to a random instance selection. A more detailed experimental setup and learning curves reporting absolute values are available in Appendix F. In general, the resulting curves confirm our hypothesis. All query strategies using our updates outperform the respective top- b selection strategies. Furthermore, combining our update with the batch selection strategy Badge also results in improved accuracy. This indicates that our idea of *selecting a single instance and updating the DNN* leads to a more effective selection than using the k -means algorithm as proposed in Badge.

6 Discussion and Conclusion

In this article, we proposed a second-order Bayesian update method for DNNs based on a last-layer LAs. It provides an efficient alternative to retraining for scenarios where data arrives sequentially and immediate updates are beneficial (e.g., AL). A extensive experimental evaluation showed that the proposed updates are both fast and effective, consistently outperforming competitors. In an AL use case, we demonstrated that the proposed update can improve sequential AL selection strategies such as Margin and BALD, as well as the popular batch selection strategy Badge.

While our proposed update has been shown to work well in the context of AL, further research is needed to explore its effectiveness in other scenarios. Specifically, when working with limited computational resources, our update can offer a efficient way to improve performance [40]. In this context, we also plan to investigate the hyperparameter γ in greater depth to adapt it during the learning process. Additionally, while our updates are effective for vanilla DNNs combined with a last-layer LA, further validation is needed for more recent models. As an initial step, we took the 2D example from Section 1 and combined our update with SNGP [30], a model designed for accurate uncertainty modeling. Figure 8 shows that the resulting update is both effective and preserves SNGP’s uncertainty modeling capabilities.

Finally, we plan to utilize our updates to enhance or develop one-step-look-ahead selection strategies [44] in deep AL. As these selection strategies are based on decision theoretic principles, they naturally balance explorative and exploitative instance selection, a key challenge in AL [28]. However, the integration of these strategies into deep learning is challenging. Current research either relies on MC-based updates [50], which we have shown to be ineffective, or does not consider deep learning [23]. Our updates offer a new and effective way to combine such strategies with DNNs.

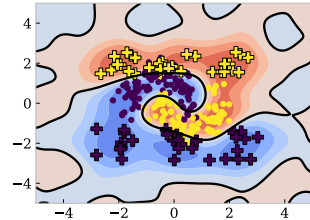


Figure 8: SNGP with our update. See Fig. 1 for the legend.

References

- [1] Jordan T. Ash, Chicheng Zhang, Akshay Krishnamurthy, John Langford, and Alekh Agarwal. Deep Batch Active Learning by Diverse, Uncertain Gradient Lower Bounds. In *International Conference on Learning Representations*, 2020.
- [2] Sören Auer, Christian Bizer, Georgi Kobilarov, Jens Lehmann, Richard Cyganiak, and Zachary Ives. Dbpedia: A nucleus for a web of open data. In *International Semantic Web Conference*, pages 722–735, 2007.
- [3] Dara Bahri, Heinrich Jiang, Tal Schuster, and Afshin Rostamizadeh. Is margin all you need? an extensive empirical study of active learning on tabular data. *arXiv preprint arXiv:2210.03822*, 2022.
- [4] Iñigo Casanueva, Tadas Temčinas, Daniela Gerz, Matthew Henderson, and Ivan Vulić. Efficient intent detection with dual sentence encoders. In *Natural Language Processing for Conversational AI*, pages 38–45, 2020.
- [5] M. Cimpoi, S. Maji, I. Kokkinos, S. Mohamed, , and A. Vedaldi. Describing textures in the wild. In *Conference on Computer Vision and Pattern Recognition*, pages 3606–3613, 2014.
- [6] Koby Crammer, Ofer Dekel, Joseph Keshet, Shai Shalev-Shwartz, and Yoram Singer. Online Passive-Aggressive Algorithms. *Journal of Machine Learning Research*, 7:551–585, 2006.
- [7] Erik Daxberger, Agustinus Kristiadi, Alexander Immer, Runa Eschenhagen, Matthias Bauer, and Philipp Hennig. Laplace redux-effortless Bayesian deep learning. In *Advances in Neural Information Processing Systems*, 2021.
- [8] Matthias De Lange, Rahaf Aljundi, Marc Masana, Sarah Parisot, Xu Jia, Aleš Leonardis, Gregory Slabaugh, and Tinne Tuytelaars. A continual learning survey: Defying forgetting in classification tasks. *Transactions on Pattern Analysis and Machine Intelligence*, 44(7):3366–3385, 2021.
- [9] Jacob Devlin, Ming-Wei Chang, Kenton Lee, and Kristina Toutanova. BERT: Pre-training of deep bidirectional transformers for language understanding. In *Conference of the North American Chapter of the Association for Computational Linguistics: Human Language Technologies*, 2019.
- [10] Alexey Dosovitskiy, Lucas Beyer, Alexander Kolesnikov, Dirk Weissenborn, Xiaohua Zhai, Thomas Unterthiner, Mostafa Dehghani, Matthias Minderer, Georg Heigold, Sylvain Gelly, Jakob Uszkoreit, and Neil Houlsby. An image is worth 16x16 words: Transformers for image recognition at scale. In *International Conference on Learning Representations*, 2021.
- [11] Sayna Ebrahimi, Mohamed Elhoseiny, Trevor Darrell, and Marcus Rohrbach. Uncertainty-guided continual learning with bayesian neural networks. In *International Conference on Learning Representations*, 2020.
- [12] Vincent Fortuin. Priors in Bayesian deep learning: A review. *International Statistical Review*, 2022.
- [13] Yarin Gal and Zoubin Ghahramani. Dropout as a Bayesian approximation: Representing model uncertainty in deep learning. In *International Conference on Machine Learning*, pages 1050–1059, 2016.
- [14] Yarin Gal, Riashat Islam, and Zoubin Ghahramani. Deep Bayesian active learning with image data. In *International Conference on Machine Learning*, pages 1183–1192, 2017.
- [15] Jakob Gawlikowski, Cedrique Rovile Njieutcheu Tassi, Mohsin Ali, Jongseok Lee, Matthias Humt, Jianxiang Feng, Anna Kruspe, Rudolph Triebel, Peter Jung, Ribana Roscher, et al. A survey of uncertainty in deep neural networks. *Artificial Intelligence Review*, 56(1):1513–1589, 2023.
- [16] Guy Hacohen, Avihu Dekel, and Daphna Weinshall. Active learning on a budget: Opposite strategies suit high and low budgets. In *International Conference on Machine Learning*, pages 8175–8195, 2022.
- [17] Steven C H Hoi, Doyen Sahoo, Jing Lu, and Peilin Zhao. Online learning: A comprehensive survey. *Neurocomputing*, 459:249–289, 2021.
- [18] Laurent Valentin Jospin, Hamid Laga, Farid Boussaid, Wray Buntine, and Mohammed Bennamoun. Hands-on Bayesian neural networks – A tutorial for deep learning users. *Computational Intelligence Magazine*, 17(2):29–48, 2022.
- [19] James Kirkpatrick, Razvan Pascanu, Neil Rabinowitz, Joel Veness, Guillaume Desjardins, Andrei A Rusu, Kieran Milan, John Quan, Tiago Ramalho, Agnieszka Grabska-Barwinska, Demis Hassabis, Claudia Clopath, Dharshan Kumaran, and Raia Hadsell. Overcoming catastrophic forgetting in neural networks. *Proceedings of the National Academy of Sciences*, 114(13):3521–3526, 2017.

[20] Andreas Kirsch, Joost Van Amersfoort, and Yarin Gal. BatchBALD: Efficient and diverse batch acquisition for deep Bayesian active learning. In *Advances in Neural Information Processing Systems*, 2019.

[21] Andreas Kirsch, Jannik Kossen, and Yarin Gal. Marginal and Joint Cross-Entropies & Predictives for Online Bayesian Inference, Active Learning, and Active Sampling. *arXiv preprint arXiv:2205.08766*, 2022.

[22] Jyrki Kivinen, Alex Smola, and Robert C Williamson. Online learning with kernels. In T. Dietterich, S. Becker, and Z. Ghahramani, editors, *Advances in Neural Information Processing Systems*, volume 14. MIT Press, 2001.

[23] Daniel Kottke, Marek Herde, Christoph Sandrock, Denis Huseljic, Georg Krempl, and Bernhard Sick. Toward optimal probabilistic active learning using a Bayesian approach. *Machine Learning*, 110(6):1199–1231, 2021.

[24] Alex Krizhevsky. Learning multiple layers of features from tiny images. Master’s thesis, University of Toronto, 2009.

[25] Balaji Lakshminarayanan, Alexander Pritzel, and Charles Blundell. Simple and scalable predictive uncertainty estimation using deep ensembles. In *Advances in Neural Information Processing Systems*, 2017.

[26] Stefan Larson, Anish Mahendran, Joseph J. Peper, Christopher Clarke, Andrew Lee, Parker Hill, Jonathan K. Kummerfeld, Kevin Leach, Michael A. Laurenzano, Lingjia Tang, and Jason Mars. An evaluation dataset for intent classification and out-of-scope prediction. In *Conference on Empirical Methods in Natural Language Processing and International Joint Conference on Natural Language Processing*, pages 1311–1316, 2019.

[27] Jeongtae Lee, Jaehong Yoon, Eunho Yang, and Sung Ju Hwang. Lifelong learning with dynamically expandable networks. *arXiv preprint arXiv:1708.01547*, 2017.

[28] Jingyao Li, Pengguang Chen, Shaozuo Yu, Shu Liu, and Jiaya Jia. Bal: Balancing diversity and novelty for active learning. *Transactions on Pattern Analysis and Machine Intelligence*, 46(5):3653–3664, 2024.

[29] Jeremiah Liu, Zi Lin, Shreyas Padhy, Dustin Tran, Tania Bedrax Weiss, and Balaji Lakshminarayanan. Simple and principled uncertainty estimation with deterministic deep learning via distance awareness. In *Advances in Neural Information Processing Systems*, 2020.

[30] Jeremiah Zhe Liu, Shreyas Padhy, Jie Ren, Zi Lin, Yeming Wen, Ghassen Jerfel, Zachary Nado, Jasper Snoek, Dustin Tran, and Balaji Lakshminarayanan. A simple approach to improve single-model deep uncertainty via distance-awareness. *Journal of Machine Learning Research*, 24(42):1–63, 2023.

[31] Liyuan Liu, Haoming Jiang, Pengcheng He, Weizhu Chen, Xiaodong Liu, Jianfeng Gao, and Jiawei Han. On the variance of the adaptive learning rate and beyond. In *International Conference on Learning Representations*, 2019.

[32] Zhiyun Lu, Eugene Ie, and Fei Sha. Mean-field approximation to Gaussian-softmax integral with application to uncertainty estimation. *arXiv preprint arXiv:2006.07584*, 2020.

[33] Matthijs. Snacks dataset. <https://huggingface.co/datasets/Matthijs/snacks>, 2021. Accessed: 2024-05-20.

[34] Takeru Miyato, Toshiki Kataoka, Masanori Koyama, and Yuichi Yoshida. Spectral normalization for generative adversarial networks. In *International Conference on Learning Representations*, 2018.

[35] Manfred Opper and Ole Winther. A Bayesian approach to on-line learning. In *On-line Learning in Neural Networks*, pages 363–378, 1999.

[36] Maxime Oquab, Timothée Darcet, Théo Moutakanni, Huy V Vo, Marc Szafraniec, Vasil Khalidov, Pierre Fernandez, Daniel HAZIZA, Francisco Massa, Alaaeldin El-Nouby, et al. DINOv2: Learning Robust Visual Features without Supervision. *Transactions on Machine Learning Research*, 2023.

[37] Yaniv Ovadia, Emily Fertig, Jie Ren, Zachary Nado, David Sculley, Sebastian Nowozin, Joshua Dillon, Balaji Lakshminarayanan, and Jasper Snoek. Can you trust your model’s uncertainty? Evaluating predictive uncertainty under dataset shift. In *Advances in Neural Information Processing Systems*, 2019.

[38] Ali Rahimi and Benjamin Recht. Random features for large-scale kernel machines. In *Advances in Neural Information Processing Systems*, 2007.

[39] Lukas Rauch, Matthias Assenmacher, Denis Huseljic, Moritz Wirth, Bernhard Bischl, and Bernhard Sick. ActiveGLAE: A Benchmark for Deep Active Learning with Transformers. In *European Conference on Machine Learning*, 2023.

[40] Lukas Rauch, Raphael Schwinger, Moritz Wirth, Bernhard Sick, Sven Tomforde, and Christoph Scholz. Active Bird2Vec: Towards End-to-End Bird Sound Monitoring with Transformers. *arXiv preprint arXiv:2308.07121*, 2023.

[41] Pengzhen Ren, Yun Xiao, Xiaojun Chang, Po-Yao Huang, Zhihui Li, Brij B. Gupta, Xiaojiang Chen, and Xin Wang. A survey of deep active learning. *Computing Surveys*, 54(9):1–40, 2021.

[42] Hippolyt Ritter, Aleksandar Botev, and David Barber. Online structured Laplace approximations for overcoming catastrophic forgetting. In *Advances in Neural Information Processing Systems*, 2018.

[43] Hippolyt Ritter, Aleksandar Botev, and David Barber. A scalable Laplace approximation for neural networks. In *International Conference on Learning Representations*, 2018.

[44] Nicholas Roy and Andrew McCallum. Toward Optimal Active Learning through Sampling Estimation of Error Reduction. In *International Conference on Machine Learning*, pages 441–448, 2001.

[45] Doyen Sahoo, Steven C.H. Hoi, and Bin Li. Online multiple kernel regression. In *Proceedings of the 20th ACM SIGKDD International Conference on Knowledge Discovery and Data Mining*, KDD ’14, page 293–302, New York, NY, USA, 2014. Association for Computing Machinery. ISBN 9781450329569. doi: 10.1145/2623330.2623712.

[46] Doyen Sahoo, Quang Pham, Jing Lu, and Steven CH Hoi. Online deep learning: learning deep neural networks on the fly. In *International Joint Conference on Artificial Intelligence*, pages 2660–2666, 2018.

[47] Ozan Sener and Silvio Savarese. Active learning for convolutional neural networks: A core-set approach. In *International Conference on Learning Representations*, 2018.

[48] Burr Settles. Active learning literature survey. Computer Sciences Technical Report 1648, University of Wisconsin–Madison, 2009.

[49] David J Spiegelhalter and Steffen L Lauritzen. Sequential updating of conditional probabilities on directed graphical structures. *Networks*, 20(5):579–605, 1990.

[50] Wei Tan, Lan Du, and Wray Buntine. Diversity enhanced active learning with strictly proper scoring rules. In *Advances in Neural Information Processing Systems*, 2021.

[51] Ben Taylor, Vicent Sanz Marco, Willy Wolff, Yehia Elkhattib, and Zheng Wang. Adaptive deep learning model selection on embedded systems. In *International Conference on Languages, Compilers, and Tools for Embedded Systems*, pages 31–43, 2018.

[52] Gido M Van de Ven, Tinne Tuytelaars, and Andreas S Tolias. Three types of incremental learning. *Nature Machine Intelligence*, 4(12):1185–1197, 2022.

[53] Hao Wang and Dit-Yan Yeung. A survey on Bayesian deep learning. *Computing Surveys*, 53(5):1–37, 2020.

[54] Thomas Wolf, Lysandre Debut, Victor Sanh, Julien Chaumond, Clement Delangue, Anthony Moi, Pierrette Cistac, Tim Rault, Remi Louf, Morgan Funtowicz, Joe Davison, Sam Shleifer, Patrick von Platen, Clara Ma, Yacine Jernite, Julien Plu, Canwen Xu, Teven Le Scao, Sylvain Gugger, Mariama Drame, Quentin Lhoest, and Alexander Rush. Transformers: State-of-the-art natural language processing. In *Conference on Empirical Methods in Natural Language Processing: System Demonstrations*, pages 38–45, 2020.

[55] Max A Woodbury. *Inverting modified matrices*. Department of Statistics, Princeton University, 1950.

[56] Byung-Jun Yoon, Xiaoning Qian, and Edward R. Dougherty. Quantifying the Objective Cost of Uncertainty in Complex Dynamical Systems. *Transactions on Signal Processing*, 61(9):2256–2266, 2013.

[57] Martin Zinkevich. Online Convex Programming and Generalized Infinitesimal Gradient Ascent. In *International Conference on Machine Learning*, 2003.

A Related Bayesian Update Methods

We formally introduce Bayesian update methods used for comparison in the main part, including Monte Carlo (MC)-based updates and our method’s simpler variant, first-order updates.

A.1 MC-based Bayesian Updates

MC-based Bayesian neural networks (BNNs) such as deep ensembles and MC-Dropout draw samples, or hypotheses, from an (approximate) posterior distribution $q(\omega|\mathcal{D})$. To obtain these samples, deep ensembles train multiple randomly initialized deep neural networks (DNNs), while MC-Dropout randomly sets a portion of parameters to zero for multiple inference steps. We refer to [15] for an in-depth explanation about these techniques.

As MC-based BNNs only have access to these samples, the idea behind the MC-based update method is to weigh these samples. More specifically, MC-based updates, as used in [50], assume a priori that every hypothesis $\omega_1, \dots, \omega_M \sim q(\omega|\mathcal{D})$ is equally likely to explain the new dataset \mathcal{D}^\oplus . Hence, the approximate distribution *over the drawn members* can be defined as a categorical distribution⁴ with parameters $\hat{\mathbf{p}} = (\hat{p}_1, \dots, \hat{p}_M)^\top$:

$$q(\omega_m|\mathcal{D}) = \text{Cat}(m|\hat{\mathbf{p}}) = \hat{p}_m = 1/M, \quad (8)$$

where M is the number of drawn ensemble members. The updated posterior distribution, which includes the new dataset \mathcal{D}^\oplus , is computed through Bayes’ theorem:

$$q(\omega_m|\mathcal{D}^\oplus, \mathcal{D}) = \text{Cat}(m|\hat{\mathbf{p}}^{\text{upd}}) \propto q(\omega_m|\mathcal{D}) \prod_{(\mathbf{x}, y) \in \mathcal{D}^\oplus} p(y|\mathbf{x}, \omega_m) \quad (9)$$

$$= \hat{p}_m \prod_{(\mathbf{x}, y) \in \mathcal{D}^\oplus} [\text{softmax}(f^{\omega_m}(\mathbf{x}))]_y = \hat{z}_m, \quad (10)$$

which is a categorical distribution with parameters $\hat{\mathbf{p}}^{\text{upd}} = (\hat{p}_1^{\text{upd}}, \dots, \hat{p}_M^{\text{upd}})^\top$ that we obtain after normalizing $\hat{\mathbf{z}} = (\hat{z}_1, \dots, \hat{z}_M)^\top$. Intuitively, the importance of each hypothesis is determined by its likelihood of explaining the new dataset \mathcal{D}^\oplus . This approximation $q(\omega_m|\mathcal{D}^\oplus, \mathcal{D})$ of the posterior distribution allows us to make new predictions by evaluating the predictive distribution from Eq. (1) accordingly:

$$p(y|\mathbf{x}, \mathcal{D}^\oplus, \mathcal{D}) = \mathbb{E}_{q(\omega|\mathcal{D}^\oplus, \mathcal{D})}[p(y|\mathbf{x}, \omega)] \approx \sum_{m=1}^M p(y|\mathbf{x}, \omega_m) \cdot q(\omega_m|\mathcal{D}^\oplus, \mathcal{D}) \quad (11)$$

$$= \sum_{m=1}^M [\text{softmax}(f^{\omega_m}(\mathbf{x}))]_y \cdot \hat{p}_m^{\text{upd}}, \quad (12)$$

which is a weighted average of the sampled hypotheses. Employing the update from Eq. (10) may lead to catastrophic forgetting. Thus, to control the influence of the new dataset \mathcal{D}^\oplus , we introduce the hyperparameter γ :

$$q(\omega_m|\mathcal{D}^\oplus, \mathcal{D}) \propto \hat{p}_m \left(\prod_{(\mathbf{x}, y) \in \mathcal{D}^\oplus} [\text{softmax}(f^{\omega_m}(\mathbf{x}))]_y \right)^\gamma. \quad (13)$$

A.2 First-Order Bayesian Updates

Our proposed update method from the main text approximates the new posterior $q(\omega|\mathcal{D}, \mathcal{D}^\oplus)$ by applying an optimization step via Gauss-Newton and estimating the new covariance. Naturally, we also introduce a first-order update, employing a first-order optimization step, leading to a less complex and faster method. This also allows us to ablate the importance of the Hessian.

Assume we have an approximate posterior distribution $q(\omega|\mathcal{D}) = \mathcal{N}(\omega|\hat{\mu}, \hat{\Sigma})$ from an LA and observe the new dataset \mathcal{D}^\oplus . Our goal is to update the approximate posterior distribution $q(\omega|\mathcal{D})$ by

⁴Equivalently, one can define the approximate distribution via multiple Dirac deltas.

considering it as the new prior distribution:

$$q(\boldsymbol{\omega} | \mathcal{D}, \mathcal{D}^\oplus) = \mathcal{N}(\boldsymbol{\omega} | \hat{\boldsymbol{\mu}}^{\text{upd}}, \hat{\boldsymbol{\Sigma}}^{\text{upd}}) \propto q(\boldsymbol{\omega} | \mathcal{D}) \prod_{(\mathbf{x}, y) \in \mathcal{D}^\oplus} p(y | \mathbf{x}, \boldsymbol{\omega}). \quad (14)$$

The first-order update is defined by using a gradient optimization step to obtain an updated mean:

$$\hat{\boldsymbol{\mu}}^{\text{upd}} = \hat{\boldsymbol{\mu}} - \gamma \left(\sum_{(\mathbf{x}, y) \in \mathcal{D}^\oplus} (\sigma(\mathbf{h}^T \hat{\boldsymbol{\mu}}) - y) \mathbf{h}_x \right), \quad (15)$$

where γ is the step size (or learning rate) introduced to avoid catastrophic forgetting. The covariance matrix must only be recomputed at the update's end if meaningful uncertainty estimates are of interest.

B Hyperparameter Ablation

For all introduced Bayesian update methods, the hyperparameter γ controls the influence of the new dataset \mathcal{D}^\oplus on the posterior distribution $q(\boldsymbol{\omega} | \mathcal{D})$. In Section 4, we conducted a small ablation study, similar to a hyperparameter search, to determine an appropriate value for γ . We intentionally did not search a optimal value of γ for every dataset since extensive hyperparameter search for update methods is impractical in an online setting [8]. Using the same setup as in Section 4, we consider the CIFAR-10 and DBpedia datasets. Our baseline DNN is trained on a randomly sampled initial dataset \mathcal{D} of 50 instances. We then update and retrain the DNN with varying sizes of the new dataset $|\mathcal{D}^\oplus| \in \{1, \dots, 10\}$.

Considering the first-order update, we see that not all values of γ improve accuracy. Especially, high values can cause a collapse in accuracy, likely due to catastrophic forgetting. We find that updates with $\gamma = 0.001$ and $\gamma = 0.01$ perform best. Since $\gamma = 0.001$ generates the highest accuracy for CIFAR-10 and does not lead to a worse performance for DBpedia, we use it for the remaining experiments. Considering MC-based update, we see that no value of gamma provides an improvement in accuracy on CIFAR-10. In contrast, for DBpedia we see that $\gamma = 0.1$ improve accuracy the most. Considering the results across datasets, we select $\gamma = 0.005$ for images and $\gamma = 0.01$ for text.

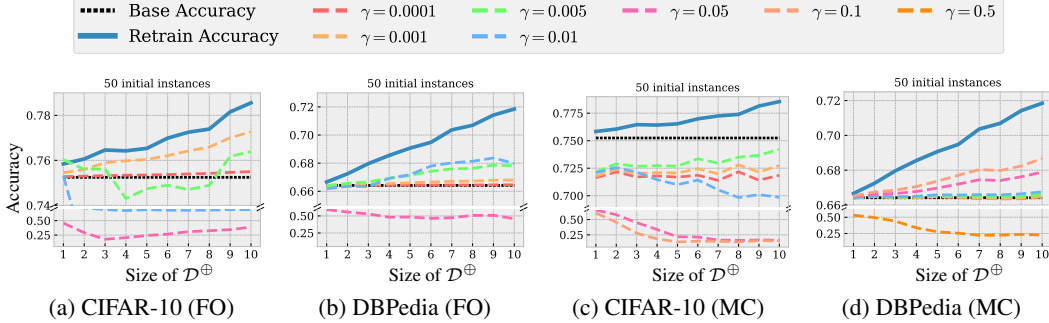


Figure 9: Accuracies after updating with different values for γ in comparison to the baseline DNN and retraining.

C Multi-class Last-Layer Update

Here, we outline three different options for performing the update step for LA in a multi-class setting with $K > 2$. In a binary setting, a last-layer LA uses a parameter vector $\boldsymbol{\omega} \in \mathbb{R}^D$. However, in a multi-class setting, we have a parameter vector $\boldsymbol{\omega}_y$ for each class $y \in \mathcal{Y}$. In the literature, several approximations haven been proposed to model these parameter vectors' distribution.

The most complex approximation would be to concatenate these vectors and model them through a multi-variate normal distribution:

$$q(\boldsymbol{\omega} | \mathcal{D}) = \mathcal{N}(\boldsymbol{\omega} | \hat{\boldsymbol{\mu}}, \hat{\boldsymbol{\Sigma}}) \text{ with } \boldsymbol{\omega}, \hat{\boldsymbol{\mu}} \in \mathbb{R}^{K \cdot D}, \hat{\boldsymbol{\Sigma}} \in \mathbb{R}^{(K \cdot D) \times (K \cdot D)}. \quad (16)$$

This approximation can estimate a covariance between each pair of parameters. However, this expressiveness comes at the cost of a large covariance matrix $\hat{\Sigma}$ to be estimated. This is particularly costly for many classes K combined with a high feature dimension D from a DNN, such that corresponding updates via second-order optimization would no longer be efficient.

Spiegelhalter and Lauritzen [49] presented a more efficient approximation in which the class-wise parameter vectors are arranged column-wisely as a matrix. Their joint distribution is then modeled through a matrix normal distribution:

$$q(\omega|\mathcal{D}) = \mathcal{MN}(\omega|\hat{\mu}, \hat{\Gamma}, \hat{\Sigma}) \text{ with } \omega, \hat{\mu} \in \mathbb{R}^{D \times K}, \hat{\Sigma} \in \mathbb{R}^{D \times D}, \hat{\Gamma} \in \mathbb{R}^{K \times K}. \quad (17)$$

This approximation captures the covariance between each pair of parameter vectors via the matrix $\hat{\Gamma}$ and each pair of hidden features via the matrix $\hat{\Sigma}$. Both matrices have to be iteratively recomputed while updating. We refer to [49] for more details.

Liu et al. [29] presented an even faster approximation and showed its effectiveness in combination with an LA for supervised learning. Therefore, we employ this approximation in the multi-class setting. The idea is to determine an upper-bound covariance matrix shared by all class-wise parameter vectors in their respective multivariate normal distribution, which is then defined for class $y \in \mathcal{Y}$ as:

$$q(\omega_y | \mathcal{D}) = \mathcal{N}(\hat{\mu}_y | \hat{\Sigma}) \text{ with } \omega_y, \hat{\mu}_y \in \mathbb{R}^D, \hat{\Sigma} \in \mathbb{R}^{D \times D}. \quad (18)$$

The upper-bound covariance matrix $\hat{\Sigma} \in \mathbb{R}^{D \times D}$ corresponds to the inverse Hessian of the negative log posterior evaluated at the MAP estimate $\hat{\mu}$ given training data \mathcal{D} and a prior covariance matrix \mathbf{I} . It is given by

$$\hat{\Sigma} = \mathbf{H}^{-1}, \text{ where } \mathbf{H} = \sum_{(\mathbf{x}, y) \in \mathcal{D}} p_{\mathbf{x}}^*(1 - p_{\mathbf{x}}^*) \mathbf{h}_{\mathbf{x}} \mathbf{h}_{\mathbf{x}}^T + \mathbf{I}, \quad (19)$$

where $p_{\mathbf{x}}^* = \max_y p(y|\mathbf{x}, \omega)$ is the maximum probability outputted by the DNN. An even simpler approximation is to assume a Gaussian likelihood for the covariance, leading to the following formulation

$$\hat{\Sigma} = \mathbf{H}^{-1}, \text{ where } \mathbf{H} = \sum_{(\mathbf{x}, y) \in \mathcal{D}} \mathbf{h}_{\mathbf{x}} \mathbf{h}_{\mathbf{x}}^T + \mathbf{I}. \quad (20)$$

which has been empirically shown to work more robustly when estimating uncertainties [30]. For this reason and its computational efficiency, we employ this approximation in our method.

Analog to the updates for binary classification in Eq. (5) and Eq.(6), we implement the updates of the mean parameter vector for class $y \in \mathcal{Y}$ and the covariance matrix $\hat{\Sigma} \in \mathbb{R}^{D \times D}$ shared across the classes \mathcal{Y} given a new dataset \mathcal{D}^{\oplus} based on the Gauss-Newton algorithm leading to:

$$\hat{\mu}_y^{\text{upd}} = \hat{\mu} - \mathbf{H}^{-1}(\hat{\mu}, \hat{\Sigma}, \mathcal{D}^{\oplus}) \sum_{(\mathbf{x}, y') \in \mathcal{D}^{\oplus}} (p_{\mathbf{x}}^* - \delta(y = y')) \mathbf{h}_{\mathbf{x}}, \quad (21)$$

$$\hat{\Sigma}^{\text{upd}} = \mathbf{H}^{-1}(\hat{\mu}^{\text{upd}}, \hat{\Sigma}, \mathcal{D}^{\oplus}), \quad (22)$$

where $\delta(\cdot)$ is the Dirac delta function. We efficiently compute the updated inverse Hessian using the Woodbury identity as presented in the upcoming Appendix D.

D Efficient Hessian Inversion via Woodbury Identity

Here, we provide the derivation of the update from Eq. (7), which uses the Woodbury (matrix) identity [55] for efficient inversion of the Hessian during updates. Assume we employed an LA and have the current approximate posterior distribution $q(\omega|\mathcal{D}) = \mathcal{N}(\omega|\hat{\mu}, \hat{\Sigma})$. To incorporate the information of the new dataset \mathcal{D}^{\oplus} into the LA's current covariance $\hat{\Sigma}$, we first need to calculate the Hessian of the new negative log posterior $q(\omega|\mathcal{D}, \mathcal{D}^{\oplus})$ with respect to ω . The Hessian of the new negative log posterior $-q(\omega|\mathcal{D}, \mathcal{D}^{\oplus})$ is given by

$$\mathbf{H} = -\nabla_{\omega}^2 \log q(\omega|\mathcal{D}, \mathcal{D}^{\oplus}) = \mathbf{I} + \sum_{(\mathbf{x}, y) \in \mathcal{D}} p_{\mathbf{x}}(1 - p_{\mathbf{x}}) \mathbf{h}_{\mathbf{x}} \mathbf{h}_{\mathbf{x}}^T + \sum_{(\mathbf{x}, y) \in \mathcal{D}^{\oplus}} p_{\mathbf{x}}(1 - p_{\mathbf{x}}) \mathbf{h}_{\mathbf{x}} \mathbf{h}_{\mathbf{x}}^T, \quad (23)$$

$$= \hat{\Sigma}^{-1} + \sum_{(\mathbf{x}, y) \in \mathcal{D}^{\oplus}} p_{\mathbf{x}}(1 - p_{\mathbf{x}}) \mathbf{h}_{\mathbf{x}} \mathbf{h}_{\mathbf{x}}^T, \quad (24)$$

where we see the updated Hessian is given by a sum of the old negative log posterior's precision matrix with the precision matrix of the new dataset \mathcal{D}^\oplus . Note, however, that we require the *inverse* Hessian \mathbf{H}^{-1} for both the Gaussian posterior in the LA and the optimization step via Gauss-Newton. Depending on the size of \mathcal{D}^\oplus and the assumed likelihood for the Hessian, this computation can significantly slow down the efficiency of our update since we must compute an inverse with each new incoming batch of instances. Thus, to ensure efficient updates, we employ the Woodbury identity, which is given in a simplified form by

$$(\mathbf{A} + \mathbf{u}\mathbf{v}^T)^{-1} = \mathbf{A}^{-1} - \frac{\mathbf{A}^{-1}\mathbf{u}\mathbf{v}^T\mathbf{A}^{-1}}{1 + \mathbf{v}^T\mathbf{A}^{-1}\mathbf{u}}, \quad (25)$$

and allows us to obtain an updated inverse Hessian directly, avoiding calculation of the inverse of the updated precision matrix. Setting $\mathbf{u} = p_{\mathbf{x}}(1 - p_{\mathbf{x}})\mathbf{h}_{\mathbf{x}}$ and $\mathbf{v} = \mathbf{h}_{\mathbf{x}}$, we obtain:

$$\mathbf{H}^{-1} = \left(\hat{\Sigma}^{-1} + p_{\mathbf{x}}(1 - p_{\mathbf{x}})\mathbf{h}_{\mathbf{x}}\mathbf{h}_{\mathbf{x}}^T\right)^{-1} = \hat{\Sigma} - \frac{p_{\mathbf{x}}(1 - p_{\mathbf{x}})}{1 + \mathbf{h}_{\mathbf{x}}\hat{\Sigma}\mathbf{h}_{\mathbf{x}} \cdot p_{\mathbf{x}}(1 - p_{\mathbf{x}})}\hat{\Sigma}\mathbf{h}_{\mathbf{x}}\mathbf{h}_{\mathbf{x}}\hat{\Sigma}, \quad (26)$$

which is the update from Eq. (7). In the multi-class setting, we employ the covariance matrix of Eq. (20) by assuming a Gaussian likelihood leading to the following inverse Hessian:

$$\mathbf{H}^{-1} = \left(\hat{\Sigma}^{-1} + \mathbf{h}_{\mathbf{x}}\mathbf{h}_{\mathbf{x}}^T\right)^{-1} = \hat{\Sigma} - \frac{\hat{\Sigma}\mathbf{h}_{\mathbf{x}}\mathbf{h}_{\mathbf{x}}\hat{\Sigma}}{1 + \mathbf{h}_{\mathbf{x}}\hat{\Sigma}\mathbf{h}_{\mathbf{x}}}, \quad (27)$$

where we set $\mathbf{u} = \mathbf{v} = \mathbf{h}_{\mathbf{x}}$.

E Summary of Datasets

CIFAR [24] consists of 60,000 colored images with a low resolution of 32×32 . There is a predetermined split of 50,000 images as training instances and 10,000 images as test instances. One variant of this dataset, **CIFAR-10**, is a coarse-grained task with ten broad classes such as automobile, dog, airplane, and ship. The classes are mutually exclusive meaning there is no overlap between, e.g., automobiles and trucks. **Snacks** [33] contains images of 20 different classes of snack foods. The 6,745 available images are split into 3,840 images for training, 955 for validation, and 920 for testing. Each image is 256 pixels wide while its height varies from 256 to 873 pixels. **DTD** [5] is a texture-focused dataset that consists of 5,640 images divided into 47 different classes. There are 120 images for each class and image sizes range between 300x300 and 640x640. There is a predetermined split into three equally sized datasets for training, validation, and testing. **DBpedia** [2] is a larger text dataset with a medium class cardinality of 14 different classes. There are 14 different ontology-based classes. It consists of 560,000 training samples and 5,000 test samples. **Banking-77** [4] comes with a more complex task of conversational language understanding alongside intent detection. The combination of its high-class cardinality and a small pool of just 10,000 samples makes this data set even more challenging. **Cline-150** [26] includes queries that are out-of-scope, i.e., queries that do not fall into any of the system's supported intents. It contains 150 in-scope intent classes, each with 100 train, 20 validation, and 30 test instances. Additionally, there are 100 train and validation out-of-scope instances, and 1,000 out-of-scope test instances.

F Active Learning: Use Case

Algorithm: The main idea from Section 5 is to transform any sequential selection strategy into a batch strategy by using the proposed update method as a fast alternative to retraining. Typically, when using a sequential selection strategy, the naive idea in a batch setting is to select the instances that resulted in the top- b highest scores, where the score is defined by the respective selection strategy. Our method can now update the DNN after each acquired label instead of selecting the top- b instances. Hence, we have a similar scenario as if we would perform single-instance acquisitions but avoid the retraining after each acquired label. After aggregating a batch of b instances, we retrain the DNN.

Algorithm 1 summarizes this idea. Given a standard AL setting with labeled data \mathcal{L} and unlabeled data \mathcal{U} , we first calculate the approximate posterior distribution $q(\omega|\mathcal{L})$ via LA. Subsequently, we iteratively select a new instance \mathbf{x} and acquire its label y based on a given selection strategy $\alpha(\cdot)$ and

Algorithm 1 Updating in AL

Require: Labeled data \mathcal{L} , unlabeled data \mathcal{U} , selection strategy α , acquisition size b , BNN $q(\omega|\mathcal{L})$

- 1: New acquisitions $\mathcal{D}^\oplus = \{\}$
- 2: **for** $i = 1, \dots, b$ **do**
- 3: Acquire next instance $\hat{x} = \text{argmax}_{x \in \mathcal{U}} \alpha(x, \mathcal{U}, q(\omega|\mathcal{D}^\oplus, \mathcal{L}))$
- 4: Obtain new label \hat{y} for instance \hat{x}
- 5: Extend new acquisitions $\mathcal{D}^\oplus \leftarrow \mathcal{D}^\oplus \cup \{(\hat{x}, \hat{y})\}$
- 6: Remove acquisition from $\mathcal{U} \leftarrow \mathcal{U} \setminus \hat{x}$
- 7: Update posterior distribution $q(\omega|\mathcal{D}^\oplus, \mathcal{L})$
- 8: **end for**
- 9: **return** Batch of new acquisitions \mathcal{D}^\oplus

update the approximate posterior distribution $q(\omega|\{(x, y)\}, \mathcal{L})$ using our method. We repeat this for b acquisitions.

Experiments: For the AL experiments in Section 5, we follow the recent work of Hacohen et al. [16]. We use the CIFAR-10 dataset and initialize the labeled pool \mathcal{L} with 10 randomly sampled instances. In each AL cycle, we select $b = 10$ new instances for labeling until a budget of $B = 200$ acquisition is reached. Each AL selection strategy selects from 1,000 randomly sampled instances from the unlabeled pool \mathcal{U} to speed up the selection process. We employ the same architecture and training hyperparameters as described in the experimental setup in Section 4.1. For the sequential selection strategies Margin [3] and Bald [14], we select batches of instances by following Algorithm 1 instead of the top- b selection. In the case of Badge [1], we replace the k -means++ algorithm that is typically used. Consequently, we select the instance with the highest gradient norm. The learning curves in Fig. 10 show that the proposed idea improves all investigated selection strategies.

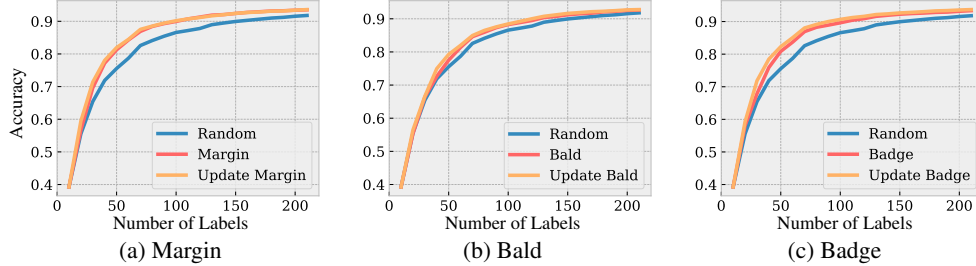


Figure 10: Learning curves reporting the accuracy of AL strategies combined with our update.